

LETTER *Special Section of Letters Selected from the 1996 IEICE General Conference*

On Unstable Saddle-Node Connecting Orbit in a Planer Autonomous System

Tetsushi UETA[†] and Hiroshi KAWAKAMI[†], *Members*

SUMMARY We found a novel connecting orbit in the averaged Duffing-Rayleigh equation. The orbit starts from an unstable manifold of a saddle type equilibrium point and reaches to a stable manifold of a node type equilibrium. Although the connecting orbit is structurally stable in terms of the conventional definition of structural stability, it is structurally unstable since a one-dimensional manifold into which the connecting orbit flows is unstable. We can consider the orbit is one of global bifurcations governing the differentiability of the closed orbit.

key words: saddle-node connecting orbit, bifurcation, topological classification of flows

1. Introduction

Generally, global bifurcations in dynamical systems are represented by the saddle-saddle connections, say homoclinic or heteroclinic orbits. As is well known, these connecting orbits are structurally unstable and behavior of an orbit near the connection can be chaotic by sufficiently small perturbations of a parameter. Therefore it is important to study the saddle-saddle connections in given nonlinear system.

We have already developed a simple method to obtain an approximate value of the parameter causing saddle-saddle connections [1], [2] and have investigated the averaged Duffing-Rayleigh (abbr. DR) or other planer autonomous systems. In this paper, we report a novel connecting orbit which is found in the averaged system. The orbit is started from an unstable manifold of the saddle and entered into the node along the eigenvector whose eigenvalue is less than the other. The orbit is structurally unstable in the sense that it is broken by the parameter perturbations.

By tracing this orbit as a bifurcation curve we obtain a bifurcation diagram with complete classification of flows in the planer parameter space. It is noteworthy that the orbit is possible in any planer autonomous system.

2. Averaged System

We treat a DR oscillator shown in Fig. 1. The differential equation of the circuit is described by the following equation:

$$\begin{aligned} \frac{d\phi}{dt} &= v \\ C \frac{dv}{dt} &= -i - g(v) + j(t) \end{aligned} \quad (1)$$

Suppose that the characteristics of a nonlinear resistor and a nonlinear inductor are as follows:

$$i_G = g(v) = -g_1 v + g_3 v^3, \quad i = f(\phi) = \frac{1}{L} \phi + \eta \phi^3 \quad (2)$$

The current source $j(t)$ supplies cosine waves:

$$j(t) = J \cos \omega t. \quad (3)$$

Let us take transformations:

$$u' = \frac{1}{\sqrt{L}} \phi, \quad v' = \sqrt{C} v, \quad \tau = \frac{1}{\sqrt{LC}} t = \omega_0 t \quad (4)$$

Consequently we have a normalized non-autonomous differential equation:

$$\begin{aligned} \dot{u}' &= v' \\ \dot{v}' &= -u' + \epsilon [(1 - \gamma v'^2) v' - c u'^3 + B \cos \nu \tau] \end{aligned} \quad (5)$$

where the dot means $d/d\tau$ and

$$\begin{aligned} \epsilon &= g_1 \sqrt{\frac{L}{C}}, \quad \gamma = \frac{g_3}{g_1 C}, \quad c = \frac{\eta L}{\omega_0 g_1} \\ B &= \frac{J \sqrt{C}}{g_1}, \quad \nu = \frac{\omega}{\omega_0}. \end{aligned} \quad (6)$$

To study the qualitative properties of the principal harmonic oscillation, we apply the averaging method to Eq. (5). By using a periodic transformation for the principal harmonic oscillation:

$$\begin{aligned} u' &= x \cos \nu \tau + y \sin \nu \tau \\ v' &= -x \sin \nu \tau + y \cos \nu \tau \end{aligned} \quad (7)$$

we have a two-dimensional averaged system:

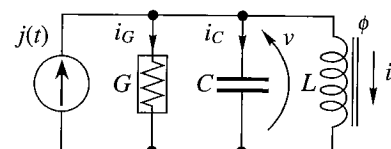


Fig. 1 Duffing-Rayleigh oscillator.

Manuscript received April 19, 1996.

[†]The authors are with the Faculty of Engineering, The University of Tokushima, Tokushima-shi, 770 Japan.

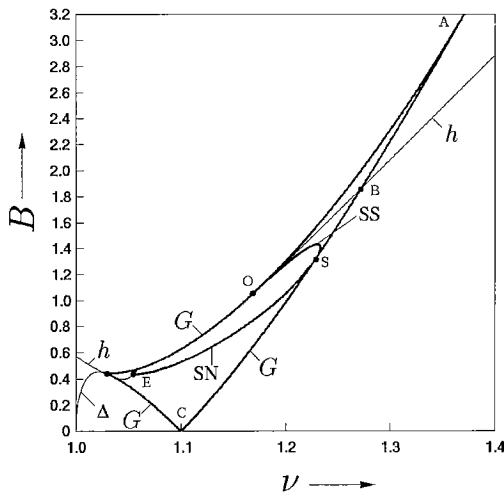


Fig. 2 Bifurcation diagram of DR equation.

$$\begin{aligned} \dot{x} &= \frac{\epsilon}{2} \left[\left(1 - \frac{3}{4}\gamma r^2\right) x - \left(\sigma - \frac{3}{4}cr^2\right) y \right] \\ \dot{y} &= \frac{\epsilon}{2} \left[\left(\sigma - \frac{3}{4}cr^2\right) x - \left(1 - \frac{3}{4}\gamma r^2\right) y + B \right] \end{aligned} \quad (8)$$

where $r = x^2 + y^2$ and $\sigma = 2(\nu - 1)/\epsilon$.

3. Bifurcations in the System

Bifurcation diagrams of some averaged systems: forced van der Pol equation discussed in Refs. [3], [4], Duffing van der Pol equation discussed in Refs. [5], [6], are similar structure of bifurcation sets. Figure 2 shows a bifurcation diagram of the equilibria and a limit cycle for Eq. (8) in ν - B space, $\epsilon = 0.2$, $c = \gamma = 1$.

Three types of bifurcations were already reported: G , h , and SS indicate saddle-node bifurcations, Hopf bifurcations, and saddle-saddle connections, respectively. The interior region surrounded by G is an entrainment domain of the principal harmonic oscillation.

There also exist codimension two bifurcations; A : cusp point connected by saddle-node bifurcations; B : simultaneous Hopf and tangent bifurcations; O : doubly degenerate equilibrium; S : saddle-node bifurcation with saddle-saddle connection in boundary of its stable manifold. These codimension two bifurcations are located in the upper-right portion of the entrainment domain. Figure 5 shows a schematic diagram enlarged from the upper-right portion of Fig. 2.

4. Unstable Saddle-Node Connecting Orbit

Now we pay attention to behavior of the orbit around the node. Let two real eigenvalues of the node be μ_1 and μ_2 , $\mu_2 < \mu_1 < 0$, and corresponding eigenvectors be ξ_1 and ξ_2 , respectively. See Fig. 3. These two eigenvectors can be regarded as stable one-dimensional manifolds. Since there exist only two orbits pass through ξ_2 , any

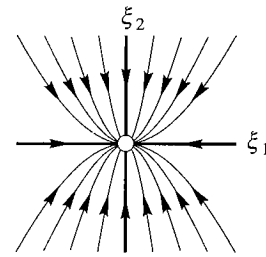


Fig. 3 A stable node.

other orbits flowing along the neighborhood of ξ_2 are attracted into ξ_1 tangentially at last [7].

We found a new type of bifurcation in Eq. (8). If an orbit approaches the saddle along its unstable manifold as $\tau \rightarrow -\infty$ asymptotically and approaches the node along the one-dimensional stable manifold ξ_2 as $\tau \rightarrow +\infty$ asymptotically, then we call this orbit *unstable saddle-node connection*. The orbit is one of unstable orbits because it is broken by the small perturbations of the system parameter, thus the existence of orbit also gives codimension one bifurcation. To prove its existence of this orbit is future objective of research. Conventionally a node is treated as a sink because it has no positive eigenvalues, thus there is no report mentioned this type of orbits.

5. Calculating Connecting Orbit

In this section, we explain briefly how to calculate the connecting orbits. The method is simple and suited to a computational algorithm because it does not require any other analytical information; using an exact solution of the system or the Melnikov method etc., so we can save time to calculate the bifurcation set.

Rewrite Eq. (8) as the following equation:

$$\dot{x} = f(x, \lambda) \quad (9)$$

where $x = (x, y)$ is a state and λ is a system parameter. Suppose that a solution of Eq. (8) is described by

$$x(\tau) = \varphi(\tau, x_0, \lambda) \quad (10)$$

where

$$x(0) = \varphi(0, x, \lambda) = x_0 \quad (11)$$

We calculate unstable saddle-node connection by Newton's method using the following conditions: Let $x_\alpha = (x_\alpha^s, y_\alpha^s)$ be a point on an unstable manifold, which has a length of δ_α from the saddle and $x_\omega = (x_\omega^n, y_\omega^n)$ be a point on a one-dimensional stable manifold ξ_2 , which has a length of δ_ω from the node. The condition of an unstable saddle-node connection is that the orbit started from x_α with forward time T_α and the orbit started from x_ω with backward time T_ω are coincided at a section Π :

$$\varphi(T_\alpha, x_\alpha, \lambda) - \varphi(-T_\omega, x_\omega, \lambda) = 0 \quad (12)$$

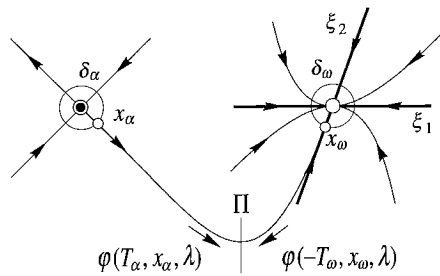


Fig. 4 A saddle-node connecting orbit.

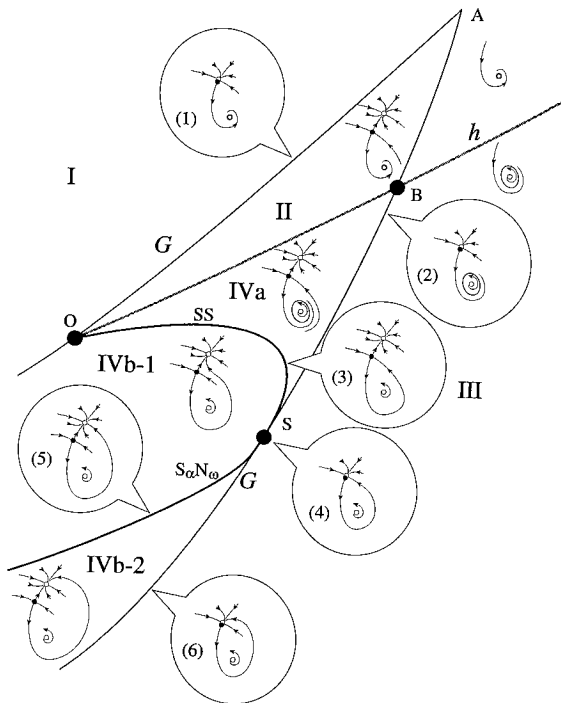


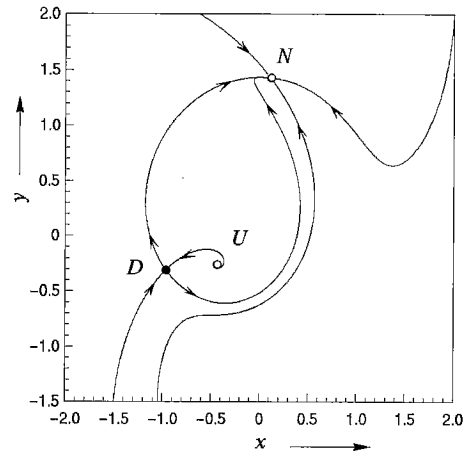
Fig. 5 Schematic bifurcation diagram. The saddle-node connecting orbit is a curve $S_{\alpha}N_{\omega}$.

Figure 4 shows a saddle-node connection. Note that this procedure is also applicable to obtain a saddle-saddle connection.

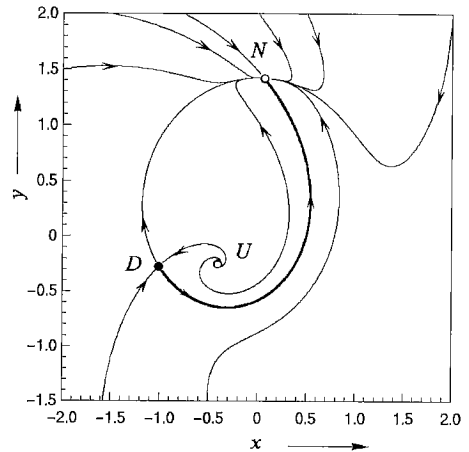
6. Classification of Flows

Bifurcation curve of the unstable saddle-node connections is shown in Figs.2 and 5 as $S_{\alpha}N_{\omega}$. This curve is started from E and terminated at S. On a curve Δ , the node is degenerated.

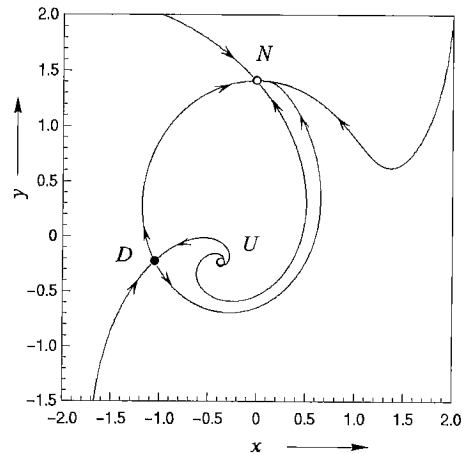
Figures 6 (a)–(c) show phase portraits when the parameter B varies across the bifurcation curve of the unstable saddle-node connection($S_{\alpha}N_{\omega}$). There are three equilibria; D : a saddle, U : a source, N : a node. Stable and unstable manifolds of the saddle D , one-dimensional manifolds of the node N , and other orbits are drawn in this figure. The thick line in Fig.6 (b) indicates an unstable saddle-node connection. It is shown



(a) $B = 0.78$



(b) $B = 0.742433$



(c) $B = 0.7$

Fig. 6 Phase portraits of the Eq. (8). $\nu = 1.15$.

that the orbit started from the unstable manifold of the saddle flips its direction of the approach to the node as B varies. Note that the saddle-node connection is structurally stable itself as a connection orbit because the it

is not disconnected by small parameter perturbations.

Figure 5 shows a schematic diagram of the upper-right portion of Fig. 2. The characteristics of flows in the regions I–IVa are topologically equivalent to the classification of the flows in an averaged van der Pol Eq. [4]. In Eq. (8), the region IVb classified in Ref. [4] is split into two parts by $S_{\alpha}N_{\omega}$. We label their two regions IVb-1 and IVb-2. Thus we can obtain a complete topological classification of flows and list out all codimension-one bifurcations in the averaged DR equation. These are sketched in balloons of Fig. 5.

Note also that the lines SS and $S_{\alpha}N_{\omega}$ approach the point S tangentially for saddle-node bifurcation G , in other words, the SS and $S_{\alpha}N_{\omega}$ bifurcations are connect at S smoothly.

These results become a help to concern differentiability of the closed loop which is composed by orbits started from the unstable manifolds of the saddle.

7. Conclusions

In this paper, we found a novel connecting orbit and calculated the bifurcation diagram of the equilibria and limit cycles in the averaged DR equation. From these results we can obtain the bifurcation diagram and topological classification of the flows completely.

To investigate a role or property of the orbit in the original DR system is a future problem.

References

- [1] H. Kawakami and Y. Katsuta, "Computation of a separatrix loop of a saddle point," *IECE Trans.*, vol.J64-A, no.10, pp. 860–861, 1981.
- [2] T. Ueta and H. Kawakami, "Heteroclinic orbits in a circuit containing a Josephson junction element," *IEICE Trans.*, vol.J-76, no.10, pp.1450–1456, 1993.
- [3] J. Guckenheimer, "Dynamics of the van der Pol equation," *IEEE Trans. Circuit & Syst.*, vol.CAS-27, no.11, 1980.
- [4] J. Guckenheimer and P. Holmes, "Nonlinear Oscillations, Dynamical Systems, and Bifurcations of Vector Fields," Springer-Verlag, 42, 1983.
- [5] Y. Ueda, "Appearance and disappearance of limit cycle correlated with the phenomenon of synchronization," *IECE Trans.* vol.J59-A, no.12, pp.1128–1130, 1976.
- [6] C. Hayashi and H. Kawakami, "Behavior of solutions for Duffing-van der Pol equation," *Proc. Int. Conf. of Nonlinear Oscillations*, Varna, 1984.
- [7] V.I. Arnold, "Ordinary Differential Equations," The MIT Press, 1973.
- [8] Y.A. Kuznetsov, "Elements of Applied Bifurcation Theory," Springer-Verlag, AMS112, 1995.